Dynamic response of spherical shells impacted by falling objects [*]

Yury A. Rossikhin, Marina V. Shitikova and Vyacheslav Shamarin

Abstract – The problem on normal low-velocity impact of an elastic falling body upon an elastic spherical shell is studied. At the moment of impact, shock waves (surfaces of strong discontinuity) are generated in the target, which then propagate along the body during the process of impact. Behind the wave fronts upto the boundary of the contact domain, the solution is constructed with the help of the theory of discontinuities and one-term or multiple-term ray expansions. Nonlinear Hertz's theory and linearized elastic contact laws are employed within the contact region. For the analysis of the processes of shock interactions of the elastic sphere or elastic spherically-headed rod with the spherical shell, nonlinear integro-differential equation has been obtained with respect to the value characterizing the local indentation of the impactor into the target, which has been solved analytically in terms of time series with integer and fractional powers. In the case of the linear elastic shock interactions, the governing differential equations for the target and the impactor are solved analytically by the ray method.

Keywords – Wave theory of impact, spherical shell, ray method, Hertz's contact law, linearized contact law, dynamic contact interaction, surface of strong discontinuity.

1 Introduction

The problems connected with the analysis of the shock interaction of thin bodies (rods, beams, plates, and shells) with other bodies have widespread application in various fields of science and technology. The physical phenomena involved in the impact event include structural responses, contact effects and wave propagation. These problems are topical not only from the point of view of fundamental research in applied mechanics, but also with respect to their applications. Because these problems belong to the problems of dynamic contact interaction, their solution is connected with severe mathematical and calculation difficulties. To overcome this impediment, a rich variety of approaches and methods have been suggested, and the overview of current results in the field can be found in recent state-of-the-art articles by Abrate [1], Rossikhin and Shitikova [2], [3] and Qatu et al. [4].

In many engineering applications, it is important to understand the transient behaviour of isotropic as well as composite thin-walled shell structures subjected to central impact by a small projectile. The problem on impact of a rigid body against an elastic spherical shell has repeatedly considered by different authors using disparate models of shock interaction [5]–[26].

Thus, Hammel [6] modeled the contact force via a spring in series with a viscous element, i.e., with a help of the Maxwell model, in so doing the local bearing of the shell's material was ignored. Later Senitskii [7] using the same problem formulation as in [6] and taking the local bearing into account studied this problem.

Using the approach which is valid for describing the shock interaction of a sphere with a infinitely stretched classical plate [27], as well as Reissner's approximate theory for transverse vibrations of shallow shells and the quasistatic Hertzian impact theory, Koller and Busenhart [8] reduced the solution of the problem of the impact response of a thin shallow spherical shell to a nonlinear integro-differential equation with respect to the value characterizing the local indentation of the spherical impactor into the shell. This equation was numerically integrated and its main results were experimentally verified.

Recently Her and Liao [16] solved the non-linear integro-differential equation derived in [8] by the numerical scheme of Runge-Kutta method to obtain the time history of the contact force at the impact point of the shell. The contact force is then applied on the apex of the shell in order to investigate the dynamic response of the shell including the displacement and stress fields by the finite element method.

Method of finite elements was adopted by Lee and Kwak [9] for the analysis of low-velocity impact of spheres on thin elastic isotropic shell structures with due account for transverse shear deformations in the target using eight-node degenerated shell element. The impact phenomenon was described by a one degree-of-freedom model based on Hertzian contact theory. The discretized nonlinear impact equations were numerically integrated using the Adams

predictor-corrector method. It has been found that the maximum contact force increases noticeably as the impact velocity of the sphere becomes higher, while the contact duration does not change considerably.

Later Liu and Swaddiwudhipong [10] generalized the approach suggested in [9] by using a nine-node degenerated shell element with assumed shear and membrane strain fields to model the laminated composite target, where the effect of large displacement and change in thickness during the impact process have been included. Both the Hertzian contact law and the modified Hertzian contact law were incorporated into the finite element program to establish the contact force history. The comparison of numerical results with those presented in [8] and [9] has exhibited reasonably good agreement.

The composite laminated shell structures subjected to low-velocity impact have been studied using ANSYS/LS-DYNA finite element software in [14]. The impact responses have been presented for the contact force and central deflection based on the modified Hertzian contact law. Numerical results have shown that structures with greater stiffness, such as smaller curvature and clamped boundary conditions, result to a larger contact force and a smaller deflection. The impact response of the structure is proportional to the impact velocity.

Damage analysis and dynamic response of elasto-plastic laminated composite shallow spherical shell under low velocity impact have been carried out by Fu et. al [**?**] and [19]. Using the classical nonlinear shell theory, a series of incremental nonlinear motion equations of orthotropic moderately thick laminated shallow spherical shell are obtained, which are solved by adopting the orthogonal collocation point method, Newmark method and iterative method synthetically. A modified elasto-plastic contact law is developed to determine the normal contact force. The effect of damage, geometrical parameters, elasto-plastic contact and boundary conditions on the contact force and the dynamic response of the structure under low velocity impact are investigated.

An approximate analytical model to predict the response of a fluid-filled spherical shell impacting by a solid elastic sphere was proposed in [13]. The model based on combining the Hertzian contact stiffness and the effective local membrane and bending stiffness was used to study the response of the human head to impact.

The nonlinear dynamic behavior of transversely isotropic shallow spherical shells on Winkler foundation subjected to impact force was studied in [20]. Based on the nonlinear theory of shallow shells, a set of nonlinear equations of motion for transversely isotropic shallow spherical shells on Winkler foundation subjected to an eccentric impact force were founded. Considering the effect of contact between the striking object and the shallow shells, using the orthogonal point collection method, the effects of striking object's initial velocity, the point of contact, Winkler foun-

dation and shell' geometrical parameters on the dynamic response of shell were discussed.

Experimental studies on dynamic behavior of thin-walled spheres in response to different impact velocity are presented in [22]. Ping pong balls are selected to study the collapse of thin-walled spheres. The tests were carried out by a modified Split Hopkinson Pressure Bar (SHPB) test system. The experimental results show that the deformation of thin-walled spherical shells depends on the impact velocity. The dynamic force in the range of small elastic deformation is larger than its quasi-static counterpart, but significantly below the latter after snap-through of the shell. The deformation and buckling mode are sensitive to the loading rate. It is noted that the strain rate effect of the materials and the inertia effect of the shell should be considered in the analysis of the shells response to dynamic loading.

A study of the collapse behaviour of hemi spherical and shallow spherical shells and their modes of deformation under impact loading are presented in [23]. Aluminium spherical shells of various radii and thicknesses were subjected to impact loading under a drop hammer and the load histories were obtained in all the cases. Three-dimensional numerical simulations were carried out for all the tested specimen geometries using LS-DYNA. Material, geometric and contact nonlinearities were incorporated in the analysis. The uni-axial stress-strain curve for the material was obtained experimentally. The results from impact experiments are used for the validation of the numerical simulations.

The normal impact of an elastic sphere upon an elastic isotropic spherical shell was also considered in [24]. The elastic features of the impactor were modeled by a linearly elastic spring, while the equations of motion of the spherical shell were adopted from the paper by Biryukov and Kadomtsev [11], who used the membrane theory of shells for describing the shock interaction of the shell with a spherical impactor.

Recently Rossikhin and Shitikova [15] have developed a new formulation of the ray method which is applicable for analyzing the propagation of surfaces of strong and weak discontinuity in thin elastic bodies when the wave fronts and the rays are referenced to the curvilinear system of coordinates. It should be noted that the ray method is primarily used for obtaining the problem solution analytically. This approach is based on the reduction of the three-dimensional equations of the dynamic theory of elasticity, which first should be written in discontinuities, to the two-dimensional equations by virtue of integration over the coordinate perpendicular to the middle surface of a thin body. The recurrent equations of this ray method are free from the shear coefficient, which is usually inherent to the Timoskenko type theories, and involve only two elastic constants: Poissons ratio and elastic modulus of elongation.

The theory proposed in [15] is applicable for short

times after the passage of the wave front, but it possesses the simplicity inherent in the "classical" theory of thin bodies. The advantages of this approach have been readily illustrated by solving the engineering problems on normal impact of an elastic thin cylindrical and spherical projectiles against an elastic spherical shell, respectively, in [25] and [26]. Nonlinear Hertz's theory was employed within the contact region, resulting in the nonlinear differential equation with respect to the value characterizing the local indentation of the impactor into the target, the analytical solution of which was found in terms of time series with integer and fractional powers. It has been shown that the contact duration and the peak of the contact force gradually decrease for increasing shell curvature. The similar conclusion concerning the contact duration can be found in [8].

In the present paper, the analytical approach proposed in [25] and in [26] for the analysis of the dynamic response of the elastic isotropic spherical shell subjected to the impact by elastic spherical and long cylindrical hemispherenose projectiles will be revised first. Then instead of the nonlinear Hertzian law we will use linearized elastic interaction law within the contact region, resulting in algebraic equations for the dsiplacements of the target and the impactor.

2 Impact response of a spherical shell of the Timoshenko type

Let an elastic sphere with the radius r_0 and mass m (Fig. 1) or a long cylindrical elastic rod of radius r_0 with a hemispherical nose of the same radius (Fig. 2) move along the x_3-axis with the velocity V_0 towards an elastic isotropic spherical shell of the R radius .

The impact occurs at the initial instant of time at $x_3 = R$. At the moment of impact, two shock wave lines (surfaces of strong discontinuity) are generated in the shell, which then propagate along the shell during the process of impact. During transition through the wave line, the following wave fields experience the discontinuities: stresses, velocities of displacements, and the values of the higher order time-derivatives in the displacements.

2.1 Geometry of the wave surface

A wave-strip is a ruled cylindrical surface consisting of the directrix C, which is the wave line propagating along the median surface of the shell, and the family of generatrices representing the line segments of the length h, which are perpendicular to the shell's median surface and thus to the wave line, and which are fitted to the wave line by their middles. Let us take the family of generatrices as the u^1-curves, where u^1 is the distance measured along the straight line segment from the C curve, and choose the distance measured along the C curve as u^2 (Fig. 3). The u^1-family
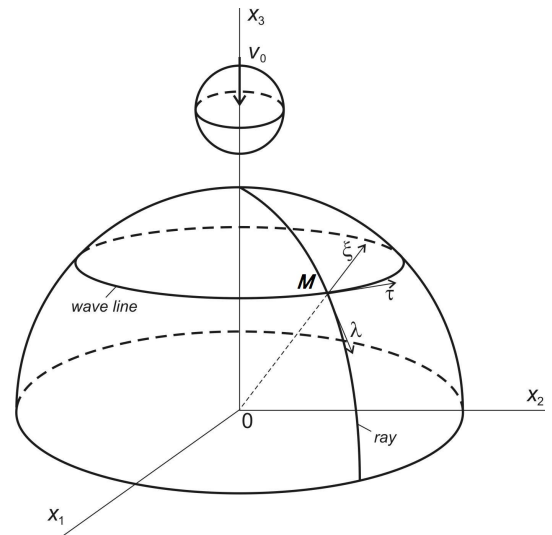

Figure 1: Scheme of the shock interaction of a falling sphere with a spherical shell

is the family of geodetic lines. In this case, all conditions of the McConnel theorem are fulfilled, and a linear element of the wave surface takes the form [28]

$$ds^2 = (du^1)^2 + g_{22}(u^1, u^2)(du^2)^2, \qquad (1)$$

in so doing

$$g_{22}(0, u^2) = 1, \qquad (2)$$

where $g_{11} = 1$, g_{22}, and $g_{12} = 0$ are the covariant components of the metric tensor of the wave surface.

The Gaussian curvature for the linear element (1) is defined by the following formula [28]:

$$K = -\frac{1}{\sqrt{g_{22}}} \frac{\partial^2 \sqrt{g_{22}}}{(\partial u^1)^2} = 0. \qquad (3)$$

Integrating Eq. (3) and considering formula (2) yields

$$\sqrt{g_{22}} = 1 + cu^1, \qquad (4)$$

where c is a certain constant.

It is known that small distances along the coordinate lines u^2 are defined by the formula [28]

$$ds_2 = \sqrt{g_{22}} \, du^2,$$

or considering (4)

$$ds_2 = (1 + cu^1)du^2. \qquad (5)$$

Let us rewrite formula (5) in the form
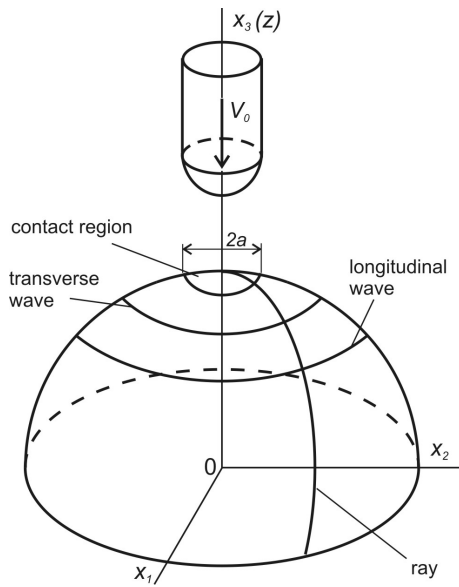
$$\frac{ds_2 - du^2}{du^2} = cu^1,$$

Figure 2: Scheme of the shock interaction of a falling cylindrical rod with a shell
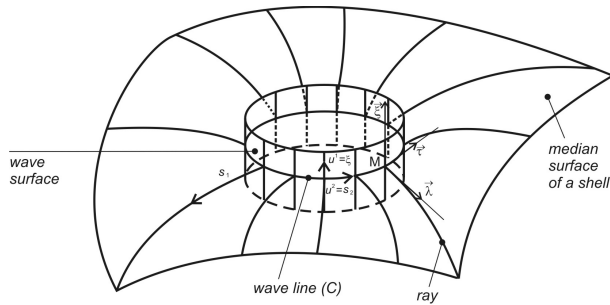

Figure 3: Scheme of the propagating wave-strip along the spherical shell surface

and integrate the result relationship with respect to u^1 from $-h/2$ to $h/2$. As a result we obtain

$$\int_{-h/2}^{h/2} \frac{ds_2 - du^2}{du^2} \, du^1 = 0,$$

or

$$\int_{-h/2}^{h/2} \frac{ds_2}{du^2} \, du^1 = h. \qquad (6)$$

Equation (6) can be written as

$$\frac{1}{h} \int_{-h/2}^{h/2} \sqrt{g_{22}} \, du^1 = 1,$$

i.e., the mean magnitude of the value $\sqrt{g_{22}}$ over the thickness of the shell is equal to unit.

If the shell's thickness is small, then it is possible to consider approximately that

$$\sqrt{g_{22}} \approx 1 \qquad (7)$$

at any point of the wave surface.

Since all values for the shell are averaged over its thickness, then such an approximation for $\sqrt{g_{22}}$ is not unreasonable.

The linear element (1) with due account for (7) can be approximately written as

$$ds^2 \approx (du^1)^2 + (du^2)^2, \qquad (8)$$

i.e., it looks like a linear element on the plane in the Cartesian set of coordinates.

Now let us define a linear element of the median surface of the shell. Since the rays intersecting the line C (the wave line) under the right angles are the family of the geodetic lines, then we once again are under the conditions of the McConnel theorem, and thus the linear element of this surface takes the form

$$ds^2 = (du_*^1)^2 + g_{22}(du^2)^2, \qquad (9)$$

but considering formula (7) it can be rewritten in the form of (8) by substituting du^1 by du_*^1.

2.2 The main kinematic and dynamic characteristics of the wave surface

Now we write the condition of compatibility on the wave surface of strong discontinuity. Based on the aforesaid and considering (7)-(9), it takes the form (see Appendix A)

$$
\begin{aligned}
[u_{i,j(k)}] &= -G^{-1}[v_{i,(k)}]\lambda_j + \frac{\delta[u_{i,(k)}]}{\delta s_1}\lambda_j \\
&+ \frac{\delta[u_{i,(k)}]}{\delta s_2}\tau_j + \left[\frac{\delta u_{i,(k)}\xi_j}{\delta \xi}\right], \qquad (10)
\end{aligned}
$$

where u_i are the displacement vector components, G is the normal velocity of the wave surface, $[u_{i,j}] = [\partial u_i/\partial x_j]$, x_j are the spatial rectangular Cartesian coordinates, $\xi = u^1$, $s_1 = u_*^1$, $[u_{i,(k)}] = [\partial^k u_i/\partial t^k]$, t is the time, $v_i = u_{i,(1)}$, λ_i, τ_i, and ξ_i are the components of the unit vectors of the tangential to the ray, the tangential to the wave surface, and the normal to the spherical surface, respectively, and Latin indices take on the values 1,2,3.

Putting $k = 0$ in (10) yields

$$[u_{i,j}] = -G^{-1}[v_i]\lambda_j + \left[\frac{\delta(u_i\xi_j)}{\delta \xi}\right]. \qquad (11)$$

Writing the Hook's law for a three-dimensional medium in terms of discontinuities and using the condition of compatibility (11), we find

$$
\begin{aligned}
[\sigma_{ij}] &= -G^{-1}\lambda[v_\lambda]\delta_{ij} - G^{-1}\mu\left([v_i]\lambda_j + [v_j]\lambda_i\right) \\
&+ \lambda[u_{\xi,\xi}]\delta_{ij} + \mu\left(\left[\frac{\delta(u_i\xi_j)}{\delta \xi} + \frac{\delta(u_j\xi_i)}{\delta \xi}\right]\right) (12)
\end{aligned}
$$

where

$$[v_\lambda] = [v_i]\lambda_i, \quad [u_{\xi,\xi}] = \left[\frac{\delta(u_i\xi_i)}{\delta \xi}\right] = \left[\frac{\delta u_\xi}{\delta \xi}\right],$$

λ and μ are Lame constants, and δ_{ij} is the Kroneker's symbol.

Multiplying relationship (12) from the right and from the left by $\xi_i \xi_j$ and considering equation

$$[\sigma_{\xi\xi}] = [\sigma_{ij}]\xi_i \xi_j = 0,$$

what corresponds to the assumption that the normal stresses on the cross-sections parallel to the middle surface could be neglected with respect to other stresses, we find

$$[u_{\xi,\xi}] = \frac{\lambda}{G(\lambda + 2\mu)}[v_\lambda]. \quad (13)$$

Multiplying relationship (12) from the right and from the left by $\lambda_i \lambda_j$, we are led to the equation

$$[\sigma_{\lambda\lambda}] = [\sigma_{ij}]\lambda_i \lambda_j = -G^{-1}(\lambda + 2\mu)[v_\lambda] + \lambda[u_{\xi,\xi}]. \quad (14)$$

Substituting (13) in (14) yields

$$[\sigma_{\lambda\lambda}] = -\frac{4\mu(\lambda + \mu)}{\lambda + 2\mu} G^{-1}[v_\lambda],$$

or

$$[\sigma_{\lambda\lambda}] = -\frac{E}{1 - \sigma^2} G^{-1}[v_\lambda], \quad (15)$$

where E and σ are the elastic modulus and the Poisson's ratio, respectively.

Alternatively, multiplying the three-dimensional equation of motion written in terms of discontinuities

$$[\sigma_{ij}]\lambda_j = -\rho G[v_i], \quad (16)$$

by λ_i, we obtain

$$[\sigma_{\lambda\lambda}] = -\rho G[v_\lambda], \quad (17)$$

where ρ is the density of the shell's material.

Eliminating the value $[\sigma_{\lambda\lambda}]$ from (15) and (17), we find the velocity of the quasi-longitudinal wave propagating in the spherical shell

$$G_1 = \sqrt{\frac{E}{\rho(1 - \sigma^2)}}. \quad (18)$$

Relationship (15) with due account for (18) takes the form

$$[\sigma_{\lambda\lambda}] = -\rho G_1[v_\lambda]. \quad (19)$$

Multiplying (12) by $\lambda_i \xi_j$ and (16) by ξ_i, we have

$$[\sigma_{\lambda\xi}] = [\sigma_{ij}]\lambda_i \xi_j = -\mu G^{-1}[v_\xi], \quad (20)$$

$$[\sigma_{\lambda\xi}] = -\rho G[v_\xi], \quad (21)$$

where $[v_\xi] = [v_i]\xi_i$.

Eliminating the value $[\sigma_{\lambda\xi}]$ from (20) and (21), we find the velocity of the quasi-transverse wave

$$G_2 = \sqrt{\frac{\mu}{\rho}}. \quad (22)$$

Considering (22), relationship (20) takes the form

$$[\sigma_{\lambda\xi}] = -\rho G_2[v_\xi]. \quad (23)$$

Note that in the three-dimensional medium only one value, i.e., $[u_{\lambda,\lambda}]$, is nonzero on the quasi-longitudinal wave, while in the two-dimensional medium, where the 'wave-strip' propagates, on the quasi-longitudinal wave there are two nonvanishing values, namely, $[u_{\lambda,\lambda}]$ and $[u_{\xi,\xi}]$. Between these two values it is possible to find the relationship. For this purpose, we multiply (11) from right and from left by $\lambda_i \lambda_j$ and express the values $[v_\lambda]$

$$[v_\lambda] = -G_1[u_{\lambda,\lambda}],$$

and then the obtained expression we substitute in (13). As a result we find the desired linkage

$$[u_{\xi,\xi}] = -\frac{\sigma}{1 - \sigma}[u_{\lambda,\lambda}]. \quad (24)$$

However, if we simply consider the strains in a thin body, for example, a plate in the rectangular Cartesian set of coordinates, assuming that

$$\sigma_{zz} = \frac{E[(1 - \sigma)u_{z,z} + \sigma(u_{x,x} + u_{y,y})]}{(1 + \sigma)(1 - 2\sigma)} = 0,$$

then it is possible to obtain a little bit another formula

$$u_{z,z} = -\frac{\sigma}{1 - \sigma}(u_{x,x} + u_{y,y}). \quad (25)$$

From the comparison of (24) and (25) it is seen that in the right-hand side of (24) the value $[u_{\tau,\tau}] = [u_{ij}]\tau_i \tau_j$ is absent, but its absence is connected with the peculiarities of the 'wave-strip', namely: it has free edges at $\xi = \pm h/2$ and a closed contour with respect to s_2.

2.3 Governing equations

Thus, behind the front of each of two transient waves (surfaces of strong discontinuity) upto the boundary of the contact domain (Fig. 1 or Fig. 2) relationships (19) and (23) are valid, which are the first terms of the ray expansions (Fig. 4), i.e.,

$$\sigma_{\lambda\lambda} = -\rho G_1 v_\lambda, \quad (26)$$

$$\sigma_{\lambda\xi} = -\rho G_2 v_\xi. \quad (27)$$

Considering the cone angle of the contact spot 2γ as a small value (Fig. 4), and putting $\cos\gamma \approx 1$, $\sin\gamma \approx \gamma = aR^{-1}$, we obtain

$$\widetilde{v_z} = \widetilde{v_\xi} - \widetilde{v_\lambda}\frac{a}{R}, \quad (28)$$
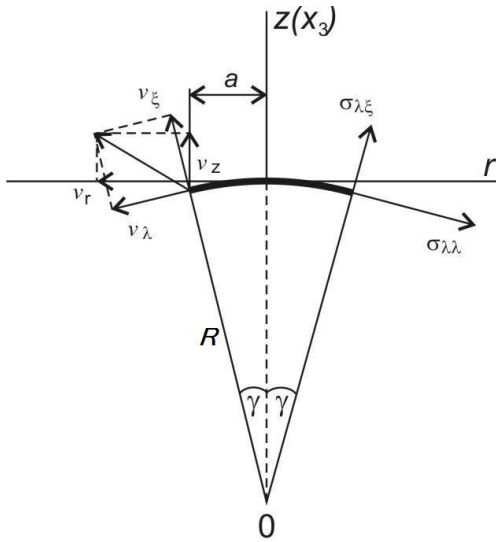
Figure 4: Scheme of velocities and stresses in the shell's element on the boundary of the contact domain

$$\widetilde{v_r} = \widetilde{v_\xi} \frac{a}{R} + \widetilde{v_\lambda}, \tag{29}$$

$$\widetilde{\sigma_{rz}} = \rho G_1 \widetilde{v_\lambda} \frac{a}{R} - \rho G_2 \widetilde{v_\xi}, \tag{30}$$

where a is the radius of the contact spot, and $\widetilde{\sigma_{rz}} = \sigma_{rz}|_{r=a}$.

According to the Hertzian theory of contact, during the loading phase the contact force F_{cont} is related to the indentation α (i.e., the difference between the displacements of impactor and target, or the local bearing of impactor and target materials), by the relationship

$$F_{\text{cont}} = k\alpha^{3/2}, \tag{31}$$

where k is the contact stiffness coefficient depending on the geometry of colliding bodies, as well as their elastic constants:

$$k = \frac{4}{3\pi} \frac{\sqrt{R'}}{k' + k''}, \quad k' = \frac{1 - \sigma^2}{E}, \quad k'' = \frac{1 - \sigma_{\text{im}}^2}{E_{\text{im}}},$$

$$\frac{1}{R'} = \frac{1}{R} + \frac{1}{r_0},$$

and σ_{im} and E_{im} are the Poisson's ratio and the Young's modulus of the impactor.

In this case, the radius of the contact zone a is connected with the relative displacement α by the following relationship:

$$a = R'^{1/2}\alpha^{1/2}. \tag{32}$$

2.4 Normal impact of an elastic sphere upon an elastic spherical shell

Let us choose a cylindrical set of coordinates $r, \theta, z = x_3$ with the center at the original point of tangency of the

sphere and the spherical shell (Fig. 2). Then the equations of motion of the sphere and the contact spot as a rigid whole in the chosen coordinate system have the form

$$m(\widetilde{v}_z + \ddot{\alpha}) = -F_{\text{cont}} \tag{33}$$

$$\rho \pi a^2 h \widetilde{v}_z = 2\pi a h \widetilde{\sigma_{rz}} + F_{\text{cont}}, \tag{34}$$

where F_{cont} is the contact force, and $\widetilde{v}_z = \dot{v}_z|_{r=a}$.

The kinematic condition

$$\widetilde{v_r} = \dot{a} \tag{35}$$

and the initial conditions

$$\alpha|_{t=0} = 0, \quad \dot{\alpha}|_{t=0} = V_0, \quad v_z|_{t=0} = 0, \tag{36}$$

where $\widetilde{v_r} = v_r|_{r=a}$, should be added to equations (33) and (34).

Integrating (33) over t and considering the initial conditions (36), we find

$$\widetilde{v}_z = -\dot{\alpha} - \frac{k}{m} \int_0^t \alpha^{3/2} dt + V_0. \tag{37}$$

Eliminating the value $\widetilde{v}_z$ from (28) and (37), we are led to one of the desired equations

$$\widetilde{v_\xi} - \widetilde{v_\lambda} \frac{a}{R} = -\dot{\alpha} - \frac{k}{m} \int_0^t \alpha^{3/2} dt + V_0. \tag{38}$$

We obtain the second desired equation if first we eliminate the value $\widetilde{v}_z$ from (33) and (34) and then exclude the value $\widetilde{\sigma_{rz}}$ from the equation found at the previous step and from (30) at a time. As a result we obtain

$$\rho G_1 \widetilde{v_\lambda} \frac{a}{R} - \rho G_2 \widetilde{v_\xi} = -\frac{1}{2} \rho a \left(\ddot{\alpha} + \frac{k}{m} \alpha^{3/2} \right)$$

$$-\frac{k}{2\pi h \sqrt{R'}} \alpha. \tag{39}$$

Solving the set of equations (38) and (39) with respect to the values $\widetilde{v_\lambda}$ and $\widetilde{v_\xi}$, we have

$$\widetilde{v_\xi} R^{-1} \sqrt{R'} \alpha = -\frac{1}{\rho(G_1 - G_2)} \left[\frac{k}{2\pi h R} \alpha^2 \right.$$

$$+ \frac{\rho R'}{2R} \alpha^{3/2} \left(\ddot{\alpha} + \frac{k}{m} \alpha^{3/2} \right)$$

$$\left. + \rho G_1 \frac{R'}{R} \alpha \left(\dot{\alpha} + \frac{k}{m} \int_0^t \alpha^{3/2} dt - V_0 \right) \right], \tag{40}$$

$$\widetilde{v_\lambda} \alpha^{1/2} = -\frac{1}{\rho(G_1 - G_2)} \left[\frac{kR}{2\pi h R'} \right.$$

$$+\frac{1}{2}\,\rho R\,\alpha^{1/2}\left(\ddot{\alpha}+\frac{k}{m}\,\alpha^{3/2}\right)\alpha$$

$$+\rho G_2\,\frac{R}{\sqrt{R'}}\left(\dot{\alpha}+\frac{k}{m}\int_0^t \alpha^{3/2}dt - V_0\right)\Bigg].\qquad(41)$$

Substituting (40) and (41) in relationship (29), which is preliminary multiplied by $\alpha^{1/2}$, and considering formula (35), we obtain the following governing nonlinear integro-differential equation with respect to the value α:

$$\left[\frac{1}{2}\,\rho\,\alpha^{1/2}\left(\ddot{\alpha}+\frac{k}{m}\,\alpha^{3/2}\right)+\frac{k}{2\pi h R'}\,\alpha\right]\left(\frac{R'}{R}\,\alpha+R\right)$$

$$+\frac{\rho}{\sqrt{R'}}\left(G_1\,\frac{R'}{R}\,\alpha+G_2 R\right)\left(\dot{\alpha}+\frac{k}{m}\int_0^t \alpha^{3/2}dt\right)$$

$$+\frac{1}{2}\,\rho(G_1-G_2)\sqrt{R'}\dot{\alpha}=\frac{\rho V_0}{\sqrt{R'}}\left(G_1\,\frac{R'}{R}\,\alpha+G_2 R\right).\qquad(42)$$

In the limiting case, when the radius of the spherical shell tents to infinity $R\to\infty$, equation (42) could be reduced to the following

$$\frac{1}{2}\,\rho\,\alpha^{1/2}\left(\ddot{\alpha}+\frac{k}{m}\,\alpha^{3/2}\right)+\frac{k}{2\pi h r_0}\,\alpha$$

$$+\frac{\rho G_2}{\sqrt{r_0}}\left(\dot{\alpha}+\frac{k}{m}\int_0^t \alpha^{3/2}dt\right)$$

$$+\frac{1}{2}\,\rho(G_1-G_2)\sqrt{r_0}\dot{\alpha}=\frac{\rho V_0 G_2}{\sqrt{r_0}}.\qquad(43)$$

We will seek a solution of (42) in the form of the following series with respect to time t:

$$\alpha=V_0 t+\sum_{i=1}^{\infty}a_i t^{(2i+1)/2}+\sum_{j=2}^{\infty}b_j t^j,\qquad(44)$$

where a_i and b_j are coefficients to be determined.

Substituting (44) into equation (42) and equating the coefficients at integer and fractional powers of t, we are led to the set of equations for defining the coefficients a_i and b_j. For example, the first three of them have the form

$$a_1=-\frac{4}{3}(G_1-G_2)\frac{V_0^{1/2}R'^{1/2}}{R}<0,$$

$$b_2=\frac{2G_2(G_1-G_2)}{R}\left(1+\frac{1}{3}\,\frac{(G_1-G_2)R'}{G_2 R}\right)>0,$$

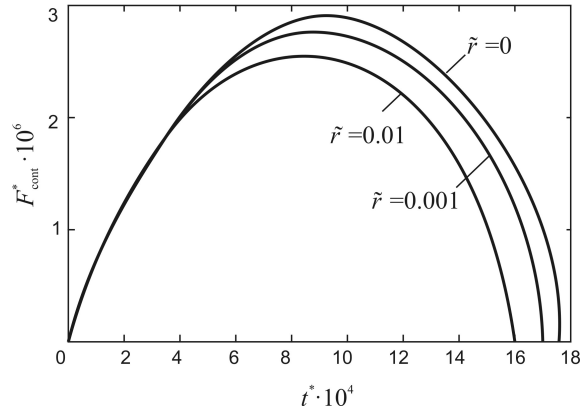$$a_2=-\frac{4}{15}\,\frac{kV_0^{1/2}}{\rho\pi h R'}-\frac{4}{15}\,V_0^{1/2}R'^{1/2}$$

Figure 5: Dimensionless time dependence of the dimensionless contact force occurring in the spherical shell impacted by the falling sphere

$$\times\left[\frac{G_2 b_2}{2V_0 R'}\left(8+\frac{1}{3}\,\frac{(G_1-G_2)R'}{G_2 R}\right)-\frac{(G_1-G_2)V_0 R'}{R^3}\right]$$

Thus, the approximate four-term solution of (42) takes the form

$$\alpha=V_0 t+a_1 t^{3/2}+b_2 t^2+a_2 t^{5/2}.\qquad(45)$$

When $R\to\infty$, the solution for equation (47) is reduced to

$$\alpha=V_0 t-\frac{4}{15}\,\frac{kV_0^{1/2}}{\rho\pi h r_0}\,t^{5/2}.\qquad(46)$$

Substituting the found function α (45), or (46) in the limiting case, in equation (31), we can obtain the final expression for the contact force.

The dimensionless time $t^*=tV_0 h^{-1}$ dependence of the dimensionless contact force $F_{\text{cont}}^*=F_{\text{cont}}(Eh^2)^{-1}$ calculated according to (31) and (45) (relationship (62) is utilized in the limiting case) is presented in Fig. 5 for the following ratios of $\tilde{r}=R_{im}/R$: 0 (what corresponds to the case of an elastic plate), 0.001, and 0.01. Reference to Fig. 5 shows that the increase in the radius of the shell results in the increase of both the contact duration and the maximum of the contact force.

2.5 Normal impact of an elastic long hemisphere-nose bar against an elastic spherical shell

At the moment of impact of a bar against a spherical shell (Fig. 2), the shock waves are generated not only in the shell but in the bar (a longitudinal shock wave) as well. This wave propagates along the bar with the velocity $G_0=\sqrt{E_{\text{im}}\rho_0^{-1}}$, where E_{im} and ρ_0 are the elastic modulus and density of the bar. Behind the front of this wave, the relationships for the stress σ^- and velocity v^- could be obtained using the ray series [2]

$$\sigma^-=-\sum_{k=0}^{\infty}\frac{1}{k!}\,[\sigma_{,(k)}]\left(t-\frac{x_3}{G_0}\right)^k,\qquad(47)$$

$$v^- = V_0 - \sum_{k=0}^{\infty} \frac{1}{k!} \left[v_{,(k)} \right] \left(t - \frac{x_3}{G_0} \right)^k. \qquad (48)$$

It is assumed that the impactor is long enough, and reflected waves do not have time to return at the place of contact before the moment of the rebound of the bar from the shell.

Considering that the discontinuities in the elastic bar remain constant during the process of the wave propagation, and using the condition of compatibility

$$G_0 \left[\frac{\partial Z_{,(k-1)}}{\partial x_3} \right] = -[Z_{,(k)}] + \frac{\delta[Z_{,(k-1)}]}{\delta t},$$

where Z is the function to be found, and $\delta/\delta t$ is the Thomas-derivative [29] , we have

$$\left[\frac{\partial \sigma_{,(k-1)}}{\partial x_3} \right] = -G_0^{-1}[\sigma_{,(k)}]. \qquad (49)$$

With due account for (49) the equation of motion on the wave surface is written in the form

$$[\sigma_{,(k)}] = -\rho_0 G_0 [v_{,(k)}]. \qquad (50)$$

Substituting (50) in (47) yields

$$\sigma^- = \rho_0 G_0 \sum_{k=0}^{\infty} \frac{1}{k!} \left[v_{,(k)} \right] \left(t - \frac{x_3}{G_0} \right)^k. \qquad (51)$$

Comparing relationships (51) and (48), we obtain

$$\sigma^- = \rho_0 G_0 (V_0 - v^-). \qquad (52)$$

At $x_3 = 0$, expression (52) takes the form

$$\sigma_{\text{cont}} = \rho_0 G_0 (V_0 - \widetilde{v}_z - \dot{\alpha}), \qquad (53)$$

where $\sigma_{\text{cont}} = \sigma^-|_{x_3=0}$ is the contact stress, $\widetilde{v}_z + \dot{\alpha} = v^-|_{x_3=0}$ is the normal velocity of the displacements of the spherical shell's points at the place of contact of the bar with the shell, α is the value characterizing the local indentation of the impactor into the shell, and an overdot denotes the time-derivative.

Using formula (53), it is possible to find the contact force

$$F_{\text{cont}} = \rho_0 G_0 (V_0 - \widetilde{v}_z - \dot{\alpha}) \pi a^2. \qquad (54)$$

However, the contact force can be determined not only by formula (54) but according the Hertz's law as well (31). Therefore

$$\pi a^2 \rho_0 G_0 (V_0 - \widetilde{v}_z - \dot{\alpha}) = k\alpha^{3/2},$$

whence it follows that

$$\widetilde{v}_z = -\dot{\alpha} - \frac{k}{\pi \rho_0 G_0 R'} \alpha^{1/2} + V_0. \qquad (55)$$

Eliminating the value $\widetilde{v}_z$ from (28) and (55), we are led to one of the desired equations

$$-\widetilde{v}_\lambda \frac{a}{R} + \widetilde{v}_\xi = -\dot{\alpha} - \frac{k}{\pi \rho_0 G_0 R'} \alpha^{1/2} + V_0. \qquad (56)$$

The second desired equation we obtain if we eliminate $\widetilde{v}_z$ and $\widetilde{\sigma}_{rz}$ from (34) by virtue of (30) and (55). As a result we obtain

$$\rho G_1 \widetilde{v}_\lambda \frac{a}{R} - \rho G_2 \widetilde{v}_\xi = \frac{1}{2} \rho a \left(-\ddot{\alpha} - \frac{k}{2\pi \rho_0 G_0 R'} \alpha^{-1/2} \dot{\alpha} \right)$$
$$- \frac{k}{2\pi h \sqrt{R'}} \alpha. \qquad (57)$$

Solving the set of equations (56) and (57) with respect to the values $\widetilde{v}_\lambda$ and $\widetilde{v}_\xi$, we have

$$\widetilde{v}_\xi R^{-1} \sqrt{R'} \, \alpha = -\frac{1}{\rho(G_1 - G_2)} \left[\frac{1}{2} \frac{\rho R'}{R} \alpha^{3/2} \left(\ddot{\alpha} \right. \right.$$
$$\left. + \frac{k}{2\pi \rho_0 G_0 R'} \alpha^{-1/2} \dot{\alpha} \right) + \frac{k}{2\pi h \sqrt{R'}} \alpha^2$$
$$\left. + \rho G_1 \frac{R'}{R} \alpha \left(\dot{\alpha} + \frac{k}{\pi \rho_0 G_0 R'} \alpha^{1/2} - V_0 \right) \right], \qquad (58)$$

$$\widetilde{v}_\lambda \alpha^{1/2} = -\frac{1}{\rho(G_1 - G_2)} \left[\frac{1}{2} \rho R \, \alpha^{1/2} \left(\ddot{\alpha} \right. \right.$$
$$\left. + \frac{k}{2\pi \rho_0 G_0 R'} \alpha^{-1/2} \dot{\alpha} \right) + \frac{kR}{2\pi h \sqrt{R'}} \alpha$$
$$\left. + \rho G_2 \frac{R}{\sqrt{R'}} \left(\dot{\alpha} + \frac{k}{\pi \rho_0 G_0 R'} \alpha^{1/2} - V_0 \right) \right]. \qquad (59)$$

Substituting (58) and (59) in (29), which is preliminary multiplied by $\alpha^{1/2}$, we obtain the governing nonlinear differential equation with respect to the value α

$$\left[\frac{1}{2} \rho \left(\alpha^{1/2} \ddot{\alpha} + \frac{k}{2\pi \rho_0 G_0 R'} \dot{\alpha} \right) + \frac{k}{2\pi h R'} \alpha \right]$$
$$\times \left(\frac{R'}{R} \alpha + R \right)$$
$$+ \frac{\rho}{\sqrt{R'}} \left(G_1 \frac{R'}{R} \alpha + G_2 R \right) \left(\dot{\alpha} + \frac{k}{2\pi \rho_0 G_0 R'} \alpha^{1/2} \right)$$
$$+ \frac{1}{2} \rho (G_1 - G_2) \sqrt{R'} \dot{\alpha} = \frac{\rho V_0}{\sqrt{R'}} \left(G_1 \frac{R'}{R} \alpha + G_2 R \right). \qquad (60)$$

In the limiting case, when the radius of the spherical shell tents to infinity $R \to \infty$, equation (60) could be reduced to the following

$$\frac{1}{2} \rho \left(\alpha^{1/2} \ddot{\alpha} + \frac{k}{2\pi \rho_0 G_0 r_0} \dot{\alpha} \right) + \frac{k}{2\pi h r_0} \alpha$$
$$+ \frac{\rho}{\sqrt{r_0}} G_2 \left(\dot{\alpha} + \frac{k}{2\pi \rho_0 G_0 r_0} \alpha^{1/2} \right) = \frac{\rho V_0}{\sqrt{r_0}} G_2. \qquad (61)$$

We will seek a solution of (60) in the form of the series (44) with respect to time t. Substituting (44) into Eq. (60) and equating the coefficients at integer and fractional powers of t, we are led to the set of equations for defining the coefficients a_i and b_j. For example, the first four of them have the form

$$a_1 = -\frac{4}{3}\left(\frac{k}{2\pi\rho_0 G_0 R'} + (G_1 - G_2)\frac{\sqrt{R'}}{R}\right)V_0^{1/2} < 0,$$

$$b_2 = \frac{3}{8}a_1^2 V_0^{-1} + G_2\left(\frac{k}{2\pi\rho_0 G_0 R'^{3/2}} + \frac{2(G_1 - G_2)}{R}\right),$$

$$\begin{aligned}
a_2 &= \frac{8}{15}\left\{\frac{1}{16}a_1 b_2 V_0^{-1} - \frac{3}{8}\frac{R'}{R^2}a_1 V_0 - \frac{kV_0^{1/2}}{2\pi\rho h R'}\right.\\
&\quad - \frac{kV_0^{1/2}}{4\pi\rho_0 G_0}\left(\frac{V_0}{R^2} + \frac{a_1 G_2}{V_0^{3/2}R'^{3/2}}\right)\\
&\quad + \left.\frac{1}{V_0^{1/2}R'^{1/2}}\left(\frac{R'}{R^2}G_1 V_0^2 - 2b_2 G_2\right)\right\},
\end{aligned}$$

$$\begin{aligned}
b_3 &= -\frac{1}{16}a_1 a_2 V_0^{-1} - \frac{3}{16}\frac{R'}{R^2}a_1^2 - \frac{1}{6}b_2^2 V_0^{-1}\\
&\quad - \frac{ka_1}{6\pi\rho h R'V_0^{1/2}} - \frac{5kV_0^{1/2}a_1}{24\pi\rho_0 G_0 R^2}\\
&\quad - \frac{1}{6V_0^{1/2}R'^{1/2}}\left(\frac{R'}{R^2}G_1 V_0^2 a_1 + 5a_2 G_2\right)\\
&\quad - \frac{k}{6\pi\rho_0 G_0 R'^{3/2}}\left(\frac{b_2 G_2}{2V_0} + \frac{R'}{R^2}G_1 V_0\right).
\end{aligned}$$

Thus, the approximate five-term solution has the form

$$\alpha = V_0 t + a_1 t^{3/2} + b_2 t^2 + a_2 t^{5/2} + b_3 t^3. \qquad (62)$$

In the limiting case, the coefficients in the series (44) representing the solution of equation (61) take the form

$$a_1 = -\frac{2}{3}\frac{kV_0^{1/2}}{\pi\rho_0 G_0 r_0} < 0,$$

$$b_2 = \frac{1}{2}\frac{k}{\pi\rho_0 G_0 r_0}\left(\frac{1}{3}\frac{k}{\pi\rho_0 G_0 r_0} + \frac{G_2}{r_0^{1/2}}\right) > 0,$$

$$a_2 = -\frac{4}{15}\frac{k}{\pi\rho_0 G_0 r_0 V_0^{1/2}}\left[\frac{2G_2^2}{r_0} + \frac{\rho_0 V_0 G_0}{\rho h}\right.$$
$$+ \left.\frac{1}{8}\frac{k}{\pi\rho_0 G_0 r_0}\left(\frac{1}{9}\frac{k}{\pi\rho_0 G_0 r_0} + \frac{3G_2}{r_0^{1/2}}\right)\right] < 0.$$

The dimensionless time $t^* = tV_0 h^{-1}$ dependence of the dimensionless contact force $F_{\text{cont}}^* = F_{\text{cont}}(Eh^2)^{-1}$ calculated according to (31) and (62) is presented in Fig.
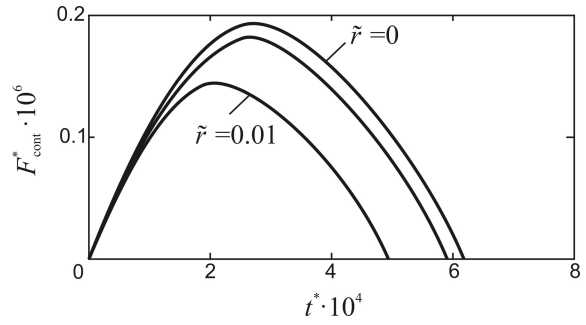
Figure 6: Dimensionless time dependence of the dimensionless contact force occurring in the spherical shell impacted by the long cylindrical rod

6 for the following ratios of $\widetilde{r} = R_{im}/R$: 0 (what corresponds to the case of an elastic plate), 0.001, and 0.01.

From Fig. 6 it is seen that the increase in the radius of the shell results in the increase of both the contact duration and the maximum of the contact force, as it has been mentioned above in the case of the dynamic response of the spherical shell impacted by the elastic sphere. However, the comparison of Figs. 5 and 6 shows that the magnitudes of the contact duration and the maximum of the contact force in the case when the spherical shell is impacted by the cylindrical rod are lower than those when the shell is impacted by the sphere. This is due to the fact that the wave phenomenon is neglected in the falling sphere, while the propagation of the transient waves in the falling rod is taken into account.

3 Impact response of a thin spherical membrane shell

Biryukov and Kadomtsev [11] suggested to determine the general displacements of the thin elastic spherical shell under the action of the force $F_{\text{cont}}(t)$ from the momentless equations of motion for spherical shells proposed in [30], which due to the symmetry of the problem under consideration and the axisymmetric character of impact loading have the following form:

$$(N_\varphi \sin\varphi)_{,\varphi} - N_\theta \cos\varphi = \rho h R \ddot{u}_\varphi \sin\varphi, \qquad (63)$$

$$N_\varphi + N_\theta = -\rho h R \ddot{w}, \qquad (64)$$

$$N_\varphi = \frac{D}{R}\left(u_{\varphi,\varphi} + w + \sigma(u_\varphi \cot\varphi + w)\right), \qquad (65)$$

$$N_\theta = \frac{D}{R}\left(u_\varphi \cot\varphi + w + \sigma(u_{\varphi,\varphi} + w)\right), \qquad (66)$$

where $D = h/k'$ is the rigidity coefficient of the shell, N_φ and N_θ are membrane forces directed along a meridian φ and a parallel θ, respectively, while its local displacements within the zone of contact of the impacting body with the shell were considered via the Hertz theory with due account for plastic deformations [11], [12] .

As it has been discussed in [2] and [31], linearization of the contact deformation is of frequent use for investigating shock interaction of solids. For the first time this approach was used in 1970 by Conway and Lee [32] for analyzing the impact between an indenter and a large elastic plate through a linear spring when investigating the mechanics of printing process. The plate was sufficiently large to ignore reflections from its boundaries, so the velocity of the contact spot was proportional to the contact force, i.e., the approach proposed by Zener [27] was valid. An elastic spring was located between the target and the indenter, so the contact force is connected with the displacements of the indenter and the contact spot (the plate's displacement at the place of contact) by a linear relationship.

Indeed, in some practical cases instead of the nonlinear Hertzian law (31) it is convenient to use the linearized contact law

$$F_{\text{cont}}(t) = E_1(\alpha - w), \qquad (67)$$

where α and w are, respectively, the displacements of the upper and lower ends of the spring with rigidity E_1, resulting in the case of an invariant contact spot (Fig. 7).

If the contact domain does not change its dimensions, then the solution of problems connected with the shock interaction of bodies is simplified significantly.

Below we shall apply this approach for describing the contact law when analyzing the impact response of the spherical membrane shell (Fig. 7).

3.1 Problem formulation and governing equations

Thus, in this case, the equation of motion of the impactor

$$m(\ddot{\alpha} + \ddot{w}) = -F_{\text{cont}}(t), \qquad (68)$$

and the equation of motion of the contact domain defined by the radius of the impactor's nose r_0

$$\rho h \pi r_0^2 \ddot{w} = 2\pi r_0 N_\varphi|_{\varphi=\varphi_0} \sin \varphi_0 + F_{\text{cont}}(t) \qquad (69)$$

subjected to the initial conditions

$$\dot{\alpha}|_{t=0} = V_0, \quad w|_{t=0} = \dot{w}|_{t=0} = 0 \qquad (70)$$

where m is the mass of the impactor, and φ_0 is the meridional coordinate of the contact spot boundary, should be added to Eqs. (63)-(66) describing the motion of the shell.

The similar approach was used in [24] for investigating the dynamic elastic response of the spherical membrane shell impacted by a sphere, however the governing Eq. (63) was written with an error, namely: the force N_θ was multiplied by $\sin \varphi$ (see Eq. (5) in [24]) instead of $\cos \varphi$.

Along with an incorrect governing equation, there is a lot of other mistakes which can be found in the cited paper by Loktev and Loktev [24], including (a) the incorrect equation of the motion of the contact domain (see Eq. (2)
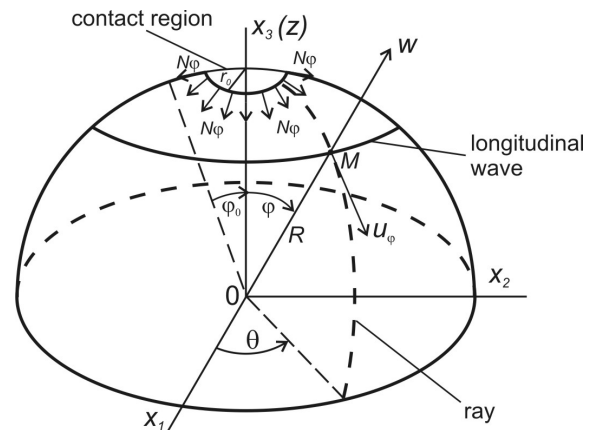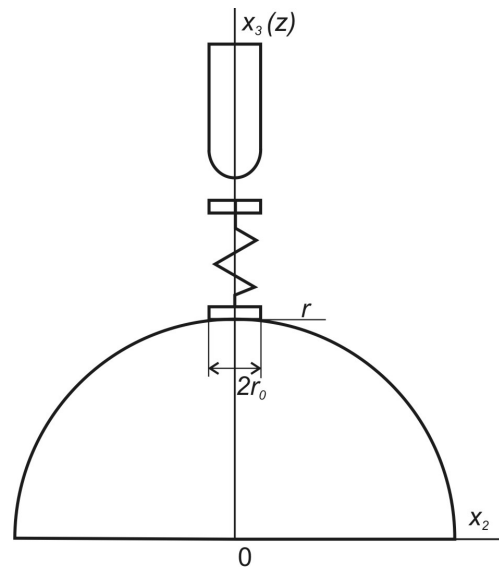

Figure 7: Scheme of the shock interaction of a hemispherical-nose impactor with a membrane shell

in [24]), wherein the meridional membrane force and circumferential membrane force acted on the contact domain boundary on its different cross sections are algebraically added and projected onto the vertical; (b) the contact force has been written as $F_{\text{cont}}(t) = E_1 \alpha$, i.e., in the form dependent only on the spring's upper end and, thus, independent of the shell's displacement; (c) faulty condition of compatibility (see Eq. (8) in [24]) which is needed for describing the longitudinal shock wave propagation during the process of impact on the basis of the theory of discontinuities. The authors of [24] have included also the boundary conditions $u_\varphi|_{\varphi=\varphi_1} = 0$ and $w|_{\varphi=\varphi_1}$ into consideration, what only misleads a reader, since under this approach they are not in use for finding the wave reflected from the simply supported boundary of the spherical panel, because it is assumed that the reflected wave comes back to

the contact domain after the re-bounce of the impactor from the target due to the significant dimensions of the spherical panel.

Such fallacies result in the final relationships for the discontinuities in the physical values to be found, where terms of different dimensions are added with each other, i.e., "kilometers" are added with "kilograms". Thus, paper by Loktev and Loktev [24] involves 21 equations in all, and only two of them, (4) and (6), are written without mistakes. The surprising thing is that this fact has not been understood by both the authors and the reviewers of this opus [24]. Moreover, it remains a mystery how the authors could carry out further the numerical investigation of such 'fantastic' relationships and present its graphical interpretation.

Since the solution of the given problem in such formulation is of certain practical interest, and its analytical results together with those obtained in the previous section could be used for the comparative analysis, then we have taken over the task of correcting all fallacies made in [24].

Below the construction of the correct solution of the problem of the shock interaction governed by Eqs. (63)-(70) is presented, resulting in the physically justified results.

3.2 Solution for the membrane spherical shell in the case of the linear contact law

Distinct from the case described in Sec. 2, the dynamic deformation of the spherical shell of the membrane type after the moment of impact $t = 0$ is governed by the longitudinal wave front of strong discontinuity which is generated in the shell in terms of the circumference propagating along the shell's middle surface with the velocity G.

Behind the front of the wave surface upto the boundary of the contact domain, a certain function $Z(\varphi, t)$ to be found could be represented by a ray series in terms of the powers of $t - R(\varphi - \varphi_0)G^{-1} > 0$ (see [2], [33])

$$Z(\varphi, t) = \sum_{k=0}^{\infty} \frac{1}{k!} [Z_{,(k)}] \left(t - \frac{R(\varphi - \varphi_0)}{G} \right)^k$$
$$\times H \left(t - \frac{R(\varphi - \varphi_0)}{G} \right), \quad (71)$$

where $[Z_{,(k)}] = [\partial^k Z / \partial t^k]$ are the jumps of the k-th order time-derivatives of the function Z, and $H(t)$ is the unit Heaviside function.

To determine coefficients of the ray series (71) for the desired functions entering in (68) and (69), we differentiate Eqs. (63)-(66) k times with respect to time, take their difference on the different sides of the wave surface, and apply the condition of compatibility [34] for discontinuities in the $k + 1$th derivatives of a certain function $Z(\varphi, t)$

$$G \left[\frac{\partial Z_{,(k)}}{\partial \gamma} \right] = -[Z_{,(k+1)}] + \frac{\delta[Z_{,(k)}]}{\delta t}, \quad (72)$$

where the curvilinear coordinate $s = R\varphi$ in the problem under consideration.

Note that the compatibility condition (72) for the components of the desired values on the curvilinear surface in the curvilinear coordinates was derived for the first time by Rossikhin and Shitikova in 1995 (see Eq. (3.1) in [34]), but for an unknown reason the first author of [24] has got himself credit for formulating this condition.

As a result of the procedure just described, we are led to the following set of the recurrent equations of the ray method:

$$\frac{R}{G} \left(1 - \frac{\rho G^2 (1 - \sigma^2)}{E} \right) [v_{\varphi(k+1)}] = 2 \frac{d[v_{\varphi(k)}]}{d\varphi}$$
$$+ \cot \varphi [v_{\varphi(k)}] + (1 + \sigma)[W_{(k)}]$$
$$- \frac{G}{R} \left\{ \frac{d^2[v_{\varphi(k-1)}]}{d\varphi^2} + \cot \varphi \frac{d[v_{\varphi(k-1)}]}{d\varphi} \right.$$
$$\left. -(\cot^2 \varphi + \sigma)[v_{\varphi(k-1)}] + (1 + \sigma) \frac{d[W_{(k-1)}]}{d\varphi} \right\}, \quad (73)$$

$$[W_{(k+1)}] = \frac{G}{R} (1 + \sigma) \Big\{ [v_{\varphi(k)}]$$
$$- \frac{G}{R} \left(\frac{d[v_{\varphi(k-1)}]}{d\varphi} + \cot \varphi [v_{\varphi(k-1)}] + 2[W_{(k-1)}] \right) \Big\}, \quad (74)$$

where $W = \dot{w}$, $v_\varphi = \dot{u}_\varphi$, and $\varphi = \varphi_0 + R^{-1}Gt$.

At $k = -1$ from Eqs. (73) and (74) we find

$$\rho G^2 = \frac{E}{1 - \sigma^2}, \qquad [W_{(0)}] = 0. \quad (75)$$

Reference to (75) shows that the velocity of the transient longitudinal wave propagating in the spherical membrane shell coincides with that for the spherical shell of the Timoshenko type, i.e., with G_1 defined by (18).

Integrating (73) at $k = 0$ yields

$$[v_{\varphi(0)}] = c_0 (\sin \varphi)^{-1/2}, \quad (76)$$

where c_0 is an arbitrary constant, but from (74) we obtain $[W_{(1)}]$ by the algebraic operation

$$[W_{(1)}] = \frac{G}{R} (1 + \sigma) c_0 (\sin \varphi)^{-1/2}. \quad (77)$$

Integrating (73) at $k = 1$ with due account for (76) and (77) yields

$$[v_{\varphi(1)}] = \left[c_1 + \frac{1}{2} \frac{G}{R} \left(\frac{3}{4} \cot \varphi + B\varphi \right) c_0 \right] (\sin \varphi)^{-1/2}, \quad (78)$$

where c_1 is an arbitrary constant, and $B = \frac{5}{4} - \sigma - (1+\sigma)^2$.

Putting $k = 1$ in (74) with due account for (76)-(78), we have

$$[W_{(2)}] = \frac{G}{R} (1 + \sigma)$$

$$\times \left[c_1 + \frac{1}{2} \frac{G}{R} \left(B\varphi - \frac{1}{4} \cot \varphi \right) c_0 \right] (\sin \varphi)^{-1/2}. \quad (79)$$

In a similar way we could find the discontinuities of the higher orders putting $k = 2$ and $k = 3$ in Eqs. (73) and (74). As a result we, respectively, obtain

$$[v_{\varphi(2)}] = \left\{ c_2 + \frac{1}{2} \frac{G}{R} \left(\frac{3}{4} \cot \varphi + B\varphi \right) c_1 \right.$$

$$+ \frac{1}{4} \frac{G^2}{R^2} \left[-\frac{15}{32} \cot^2 \varphi + \frac{5}{4} B \ln(\sin \varphi) \right.$$

$$- \frac{1}{2} B\varphi \cot \varphi - \frac{5}{4} B \left(\varphi - \frac{\varphi^3}{9} - \frac{\varphi^5}{225} \right)$$

$$\left. \left. - B \left(\sigma + (1 + \sigma)^2 \right) \frac{\varphi^2}{2} \right] c_0 \right\} (\sin \varphi)^{-1/2}, \quad (80)$$

$$[W_{(3)}] = \frac{G}{R} (1 + \sigma) \left\{ c_2 + \frac{1}{2} \frac{G}{R} \left(B\varphi - \frac{1}{4} \cot \varphi \right) c_1 \right.$$

$$+ \frac{G^2}{R^2} \left[\frac{3}{8} \left(1 + \frac{3}{16} \cot^2 \varphi \right) \right.$$

$$+ \frac{5}{16} B \ln(\sin \varphi) - \frac{1}{2} B \left(1 + \frac{3}{4} \varphi \cot \varphi \right)$$

$$- \frac{5}{16} B \left(\varphi - \frac{\varphi^3}{9} - \frac{\varphi^5}{225} \right) - 2(1 + \sigma)$$

$$\left. \left. - \frac{1}{4} B \left(\sigma + (1 + \sigma)^2 \right) \frac{\varphi^2}{2} \right] c_0 \right\} (\sin \varphi)^{-1/2}, \quad (81)$$

$$[v_{\varphi(3)}] = \left\{ c_3 + \frac{1}{2} \frac{G}{R} \left(\frac{3}{4} \cot \varphi + B\varphi \right) c_2 \right.$$

$$+ \frac{1}{4} \frac{G^2}{R^2} \left[-\frac{15}{32} \cot^2 \varphi + \frac{5}{4} B \ln(\sin \varphi) \right.$$

$$- \frac{1}{2} B\varphi \cot \varphi - \frac{5}{4} B \left(\varphi - \frac{\varphi^3}{9} - \frac{\varphi^5}{225} \right)$$

$$\left. \left. - B \left(\sigma + (1 + \sigma)^2 \right) \frac{\varphi^2}{2} \right] c_1 \right\} (\sin \varphi)^{-1/2}, \quad (82)$$

$$[W_{(4)}] = \frac{G}{R} (1 + \sigma) \left\{ c_3 + \frac{1}{2} \frac{G}{R} \left(B\varphi - \frac{1}{4} \cot \varphi \right) c_2 \right.$$

$$+ \frac{G^2}{R^2} \left[\frac{3}{8} \left(1 + \frac{3}{16} \cot^2 \varphi \right) \right.$$

$$+ \frac{5}{16} B \ln(\sin \varphi) - \frac{1}{2} B \left(1 + \frac{3}{4} \varphi \cot \varphi \right)$$

$$- \frac{5}{16} B \left(\varphi - \frac{\varphi^3}{9} - \frac{\varphi^5}{225} \right) - 2(1 + \sigma)$$

$$\left. \left. - \frac{1}{4} B \left(\sigma + (1 + \sigma)^2 \right) \frac{\varphi^2}{2} \right] c_1 \right\} (\sin \varphi)^{-1/2}, \quad (83)$$

where c_2 and c_3 are arbitrary constants to be determined from the boundary conditions. In Eqs. (82) and (83), the terms involving the constant c_0 are omitted, since it will be shown below that this constant vanishes.

Along with the discontinuities in the velocities of displacements, we should find the discontinuities in the meridional membrane force N_φ entering into the equation of the contact domain motion (69). For this purpose we rewrite Eq. (65) in the discontinuities using the condition of compatibility (71)

$$[N_{\varphi(k)}] = \frac{D}{R} \left\{ -\frac{R}{G} [v_{\varphi(k)}] + \frac{d[v_{\varphi(k-1)}]}{d\varphi} \right.$$

$$\left. + \sigma \cot \varphi [v_{\varphi(k-1)}] + (1 + \sigma)[W_{(k-1)}] \right\} \quad (84)$$

whence it follows at $k = 0$ and $k = 1$

$$[N_{\varphi(0)}] = -\rho G h c_0 (\sin \varphi)^{-1/2}, \quad (85)$$

$$[N_{\varphi(1)}] = -\rho G h (\sin \varphi)^{-1/2}$$

$$\times \left[c_1 + \frac{G}{R} \left\{ \left(\frac{7}{8} - \sigma \right) \cot \varphi + \frac{1}{2} B\varphi \right\} c_0 \right], \quad (86)$$

$$[N_{\varphi(2)}] = -\rho G h (\sin \varphi)^{-1/2}$$

$$\times \left[c_2 + \frac{G}{R} \left\{ \left(\frac{7}{8} - \sigma \right) \cot \varphi + \frac{1}{2} B\varphi \right\} c_1 \right]. \quad (87)$$

Thus, the four-term truncated ray series for the desired values on the boundary of the contact domain at $\varphi = \varphi_0$ take the form

$$N_\varphi = [N_{\varphi(0)}]|_{\varphi=\varphi_0} + [N_{\varphi(1)}]|_{\varphi=\varphi_0} t + [N_{\varphi(2)}]|_{\varphi=\varphi_0} \frac{t^2}{2}$$

$$+ [N_{\varphi(3)}]|_{\varphi=\varphi_0} \frac{t^3}{6}, \quad (88)$$

$$W = [W_{(1)}]|_{\varphi=\varphi_0} t + [W_{(2)}]|_{\varphi=\varphi_0} \frac{t^2}{2} + [W_{(3)}]|_{\varphi=\varphi_0} \frac{t^3}{6}$$

$$+ [W_{(4)}]|_{\varphi=\varphi_0} \frac{t^4}{24}. \quad (89)$$

Representing the value α in terms of the power series in time t

$$\alpha = \alpha_1 t + \alpha_2 t^2 + \alpha_3 t^3 + \alpha_4 t^4 + \alpha_5 t^5, \quad (90)$$

where α_i $(i = 1, 2, ..., 5)$ are constants to be determined, substituting (88)-(90) into Eqs. (68) and (69) with due account for (67) and the initial conditions (70), and equating the coefficients at equal powers of t in the relationships obtained, we could determine all desired constants

$$c_0 = 0, \qquad c_1 = \frac{E_1 V_0 R (\sin \varphi_0)^{1/2}}{MG(3 + \sigma)}, \quad (91)$$

$$c_2 = -\frac{G}{R}\left[\frac{1}{2}B\varphi_0 + \left(\frac{2(1-\sigma)}{3+\sigma} - \frac{1}{8}\right)\cot\varphi_0\right]c_1,$$

$$c_3 = -E_1 c_1\left[\frac{1}{m} + \frac{2(1+\sigma)}{M(3+\sigma)}\right]$$

$$+\frac{G^2}{R^2}\left\{\left[\frac{1}{2}B\varphi_0 + \left(\frac{2(1-\sigma)}{3+\sigma} - \frac{1}{8}\right)\cot\varphi_0\right]^2\right.$$

$$-\frac{5}{16}B\ln(\sin\varphi_0) + \frac{5}{16}B\left(\varphi_0 - \frac{\varphi_0^3}{9} - \frac{\varphi_0^5}{225}\right)$$

$$+\frac{1}{4}B\left(\sigma + (1+\sigma)^2\right)\frac{\varphi_0^2}{2} - \frac{3}{8}\left(1 + \frac{3}{16}\cot^2\varphi_0\right)$$

$$+\frac{1}{2}B\left(1 + \frac{3}{4}\varphi_0\cot\varphi_0\right) + 2(1+\sigma)$$

$$-\frac{1-\sigma}{3+\sigma}\left[\frac{3}{4}\cot^2\varphi_0 + B\varphi_0\cot\varphi_0 + 2(1+\sigma)\right]\Bigg\}c_1,$$

$$\alpha_1 = V_0, \quad \alpha_2 = 0, \tag{92}$$

$$6\alpha_3 = -E_1 V_0\left[\frac{1}{m} + \frac{1+\sigma}{M(3+\sigma)}\right] < 0,$$

$$12\alpha_4 = \frac{E_1 V_0(1-\sigma^2)\cot\varphi_0}{M(3+\sigma)}\frac{G}{R} > 0,$$

$$120\alpha_5 = E_1^2 V_0\left[\frac{1}{m} + \frac{1+\sigma}{M(3+\sigma)}\right]\left[\frac{1}{m} + \frac{2(1+\sigma)}{M(3+\sigma)}\right]$$

$$-\frac{E_1 V_0}{M}\frac{(1-\sigma^2)}{(3+\sigma)^2}\frac{G^2}{R^2}\left[\left(\frac{1-\sigma}{3+\sigma} + \frac{1}{8}\right)\cot^2\varphi_0\right.$$

$$\left.-2(1+\sigma) - \frac{1}{2}B\varphi_0\cot\varphi_0\right],$$

where $M = \rho h\pi r_0^2$ is the mass of the contact domain.

Now substituting the found values in Eq. (67), we can write the relationship for the contact force

$$F_{\text{cont}}(t) = E_1 V_0\left\{t - E_1\left[\frac{1}{m} + \frac{2(1+\sigma)}{M(3+\sigma)}\right]\frac{t^3}{6}\right. \tag{93}$$

$$+\frac{E_1 G(1-\sigma^2)\cot\varphi_0}{MR(3+\sigma)^2}\frac{t^4}{6} + E_1\left[E_1\left(\frac{1}{m} + \frac{2(1+\sigma)}{M(3+\sigma)}\right)^2\right.$$

$$\left.+\frac{2G^2(1-\sigma)^2}{MR^2(3+\sigma)^2}\left(\frac{5\sigma-1}{3+\sigma}\cot^2\varphi_0 + 2(1+\sigma)\right)\right]\frac{t^5}{120}\Bigg\},$$

and for the dynamic deflection of the shell at the place of the contact interaction

$$w(t) = \frac{E_1 V_0(1+\sigma)}{M(3+\sigma)}\left\{\frac{t^3}{6} - \frac{G(1-\sigma)\cot\varphi_0}{R(3+\sigma)}\frac{t^4}{12}\right. \tag{94}$$

$$-\left[E_1\left(\frac{1}{m} + \frac{2(1+\sigma)}{M(3+\sigma)}\right)\right.$$

$$\left.+\frac{G^2(1-\sigma)}{R^2(3+\sigma)}\left(\frac{5\sigma-1}{3+\sigma}\cot^2\varphi_0 + 2(1+\sigma)\right)\right]\frac{t^5}{120}\Bigg\}.$$
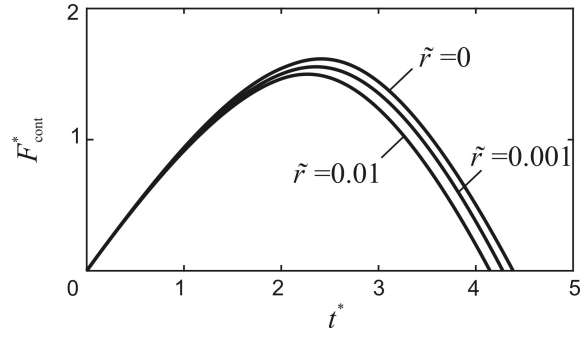
Figure 8: Dimensionless time dependence of the dimensionless contact force during the impact response of the spherical membrane shell

Putting $F_{\text{cont}}(t) = 0$ in Eq. (93), we can estimate the duration of the contact interaction

$$t_{\text{cont}} = \sqrt{\frac{6}{E_1}\left[\frac{1}{m} + \frac{2(1+\sigma)}{M(3+\sigma)}\right]^{-1}} \tag{95}$$

From Eq. (93) it follows that the contact force attains its maximal value

$$F_{\text{cont}}^{\max}(t_{\max}) = \frac{2}{3}E_1 V_0 t_{\max} \tag{96}$$

at the instant of time $t = t_{\max} = \frac{\sqrt{3}}{3}t_{\text{cont}}$.

The dimensionless time $t^* = tV_0 h^{-1}$ dependence of the dimensionless contact force $F_{\text{cont}}^* = F_{\text{cont}}(E_1 R_{\text{im}})^{-1}$ calculated according to (93) is presented in Fig. 8 for the following ratios of $\widetilde{r} = R_{im}/R$: 0 (what corresponds to the case of an elastic plate), 0.001, and 0.01.

From Fig. 8 it is seen that the increase in the radius of the shell results in the increase of both the contact duration and the maximum of the contact force, i.e., the behaviour of these curves is similar to those for the Timoshenko type spherical shell (Figs. 5 and 6), but here the influence of the shell radius is rather weak, while the magnitudes of the contact duration and the maximum of the contact force for the membrane shell are greater than those for the Timoshenko type spherical shell due to the membrane's high flexibility.

4 Conclusion

The problem on normal low-velocity impact of an elastic falling body upon an elastic spherical shell has been analyzed using the wave approach. Two theories of elastic shells have been employed: the Timoshenko-type spherical shell and membrane-type spherical shell. At the moment of impact, shock waves (surfaces of strong discontinuity) are generated in the target, which then propagate along the body during the process of impact. In the case of the Timoshenko-type shell there are two transient waves: quasi-longitudinal and quasi-transverse waves, while in the

case of the membrane-type shell there is only one shock longitudinal wave. Behind the wave fronts upto the boundary of the contact domain, the solution is constructed with the help of the theory of discontinuities and one-term or multiple-term ray expansions.

Nonlinear Hertz's theory and linearized elastic contact laws are employed within the contact region, respectively, for the Timoshenko-type and membrane-type spherical elastic shells. For the analysis of the processes of shock interactions of the elastic sphere or elastic spherically-headed rod with the Timoshenko-type spherical shell, nonlinear integro-differential or nonlinear differential equations have been ,respectively, obtained with respect to the value characterizing the local indentation of the impactor into the target, which have been solved analytically in terms of time series with integer and fractional powers. In the case of the linear elastic shock interaction, the governing linear differential equations for the membrane-type spherical shell and the impactor are solved analytically by the ray method.

Numerical calculations show that the increase in the radius of the shell results in the increase of both the contact duration and the maximum of the contact force for all types of the impactor and irrespectively of the shell's theory. However, the type of the impactor or the kind of the shell equations influence greatly on the magnitudes of the contact duration and the maximum which the contact force could attain during the process of the contact interaction. The shortest time of the contact interaction is seen when the cylindrical rod is taken as the impactor, since in this case the wave propagation phenomenon is taken into account in both interacting bodies. The largest duration takes place when the membrane-type spherical shell is utilized as the target due to its high compliance as compared with the Timoshenko-type spherical shell theory.

References:

[1] S. Abrate, "Modeling of impacts on composite structures," *Composite Structures*, vol. 51, pp. 129–138, 2001.

[2] Yu. A. Rossikhin and M. V. Shitikova, "Transient response of thin bodies subjected to impact: Wave approach," *Shock and Vibration Digest*, vol. 39, pp. 273–309, 2007.

[3] Yu. A. Rossikhin and M. V. Shitikova, "Application of fractional calculus for dynamic problems of solid mechanics: Novel trends and recent results," *Applied Mechanics Reviews*, vol. 63(1), pp. 010801-1–52, 2010.

[4] M. S. Qatu, R. W. Sullivan and W. Wang, "Recent research advances on the dynamic analysis of composite shells: 2000–2009," *Composite Structures*, vol. 93, pp. 14–31, 2010.

[5] J. C. S. Yang, "Impact on plates and shells," *International Journal of Solids and Structures*, vol. 7, pp. 445–458, 1971.

[6] J. Hammel, "Aircraft impact on a spherical shell," *Nuclear Engineering and Design*, vol. 37, pp. 205–223, 1976.

[7] Yu. E. Senitskii, "Impact of a viscoelastic solid along a shallow spherical shell," *Mechanics of Solids* (English translation), vol. 17, pp. 120–124, 1982.

[8] M. G. Koller and M. Busenhart, "Elastic impact of spheres on thin shallow spherical shells," *International Journal of Impact Engineering*, vol. 4, pp. 11–21, 1986.

[9] D. I. Lee and B. M. Kwak, "An analysis of low-velocity impact of spheres on elastic curved-shell structures," *International Journal of Solids and Structures*, vol. 30, pp. 2879–2893, 1993.

[10] Z. Liu and S. Swaddiwudhipong, "Response of plate and shell structures due to low velocity impact," *ASCE Journal of Engineering Mechanics*, vol. 123, pp. 1230–1237, 1997.

[11] D. G. Biryukov and I. G. Kadomtsev, "Dynamic elastoplastic interaction between an impactor and a spherical shell," *Journal of Applied Mechanics and Technical Physics* (English translation), vol. 43, pp. 777–781, 2002.

[12] D. G. Biryukov and I. G. Kadomtsev, "Nonaxisymmetric elastoplastic impact of a parabolic body on a spherical shell," *Journal of Applied Mechanics and Technical Physics* (English translation), vol. 46, pp. 148–152, 2005.

[13] P. G. Young, "An analytical model to predict the response of fluid-filled shells to impact – a model for blunt head impacts," *Journal of Sound and Vibration*, vol. 267, pp. 1107–1126, 2003.

[14] S.-C. Her and Y.-C. Liang, "The finite element analysis of composite laminates and shell structures subjected to low velocity impact," *Composite Structures*, vol. 66, pp. 277–285, 2004.

[15] Yu. A. Rossikhin and M. V. Shitikova, "The method of ray expansions for investigating transient wave processes in thin elastic plates and shells," *Acta Mechanica*, vol. 189, pp. 87–121, 2007.

[16] S.-C. Her and C.-C. Liao, "Analysis of elastic impact on thin shell structures. *International Journal of Modern Physics B*, vol. 22, pp. 1349–1354, 2008.

[17] Y. Fu and Y. Mao, "Nonlinear dynamic response for shallow spherical moderate thick shells with damage under low velocity impact (in Chinese)," *Acta Materiale Compositae Sinica*, vol. 25, pp. 166–172, 2008.

[18] Y. Fu, Z. Gao, and J. Yang, "Nonlinear dynamic response for transversely isotropic shallow spherical shells under impact (in Chinese)," *Chinese Journal of Applied Mechanics*, vol. 25(1), pp. 6–10, 2008.

[19] Y. Fu, Y. Mao, and Y. Tian, "Damage analysis and dynamic response of elasto-plastic laminated composite shallow spherical shell under low velocity impact, *International Journal of Solids and Structures*, vol. 47, pp. 126–137, 2010.

[20] M.-C. Wen and Z.-D. Dai, "Dynamic analysis of transversely isotropic shallow spherical shells of Winkler foundation subjected to impact force (in Chinese), *Zhongnan Daxue Xuebao (Ziran Kexue Ban)/Journal of Central South University (Science and Technology)*, vol. 39, pp. 629–634, 2008.

[21] V.X. Kunukkasseril and R. Palaninathan, "Impact experiments on shallow spherical shells," *Journal of Sound and Vibration*, vol. 40, pp. 101–107, 1975.

[22] X. L. Dong, Z. Y. Gao, and T. X. Yu, "Dynamic crushing of thin-walled spheres: An experimental study," *International Journal of Impact Engineering*, vol. 35, pp. 717–726, 2008.

[23] N. K. Gupta, N. Mohamed Sheriff, and R. Velmurugan, "Experimental and numerical investigations into collapse behaviour of thin spherical shells under drop hammer impact," *International Journal of Solids and Structures*, vol. 44, pp. 3136–3155, 2007.

[24] A. A. Loktev and D. A. Loktev, "Transverse impact of a ball on a sphere with allowance for waves in the target," *Technical Physics Letters* (English translation), vol. 34, pp. 960–963, 2008.

[25] Yu. Rossikhin and M. Shitikova, "Dynamic response of a spherical shell impacted by an elastic rod with a rounded end," in *Latest Trends on Engineering Mechanics, Structures, Engineering Geology*, Proc. of the 3rd WSEAS Int. Conf. EMESEG'10, WSEAS Press, ISBN 978-960-474-203-5, 2010, pp. 453–458.

[26] Yu. Rossikhin, M. Shitikova, and V. Shamarin, "Dynamic response of a spherical shell impacted by a sphere," in *Recent Research in Hydrology, Geology and Continuum Mechanics*, Proc. of the 6th IASME/WSEAS Int. Conf. on Continuum Mechanics (CM'11), WSEAS Press, ISBN 978-960-474-275-2, 2011, pp. 51–56.

[27] C. Zener, "The intrinsic inelasticity of large plates," *Physical Reviews*, vol. 59, pp. 669–673, 1941.

[28] A.J. McConnel, *Application of Tensor Analysis*. Dover Publications, New York, 1957.

[29] T.Y. Thomas, *Plastic Flow and Fracture in Solids*. Academic Press, New York, 1961.

[30] A.L. Goldenveizer, *Theory of Elastic Thin Shells* (in Russian). Gostekhizdat, Moscow, 1953.

[31] S. Abrate, "Localized impact on sandwich structures with laminated facing," *Applied Mechanics Reviews*, vol. 50, pp. 69–82, 1997.

[32] H.D. Conway and H.C. Lee, "Impact of an indenter on a large plate," *ASME Journal of Applied Mechanics*, vol. 37, pp. 234–235, 1970.

[33] Yu. A. Rossikhin and M. V. Shitikova, "A ray method of solving problems connected with a shock interaction," *Acta Mechanica*, vol. 102, pp. 103–121, 1994.

[34] Yu. A. Rossikhin and M. V. Shitikova, "The ray method for solving boundary problems of wave dynamics for bodies having curvilinear anisotropy," *Acta Mechanica*, vol. 109, pp. 49–64, 1995.

Appendix A

The condition of compatibility (10) could be obtained on the basis of the following reasoning. The wave line C in the reality is a very thin cylindrical 'surface-strip' (Fig. 3), for which the wave line C is served as its directrix, and the family of generatrices representing the line segments of the length h, which are perpendicular to the shell's median surface and thus to the wave line, and which are fitted to the wave line by their middles. On the wave line of strong discontinuity, there exist two conditions of compatibility for the desired values [29]:

the kinematic condition of compatibility

$$\frac{\delta[f]}{\delta t} = \left[\frac{\partial f}{\partial t}\right] + \left[\frac{df}{dn}\right] G, \qquad (A1)$$

and the geometric condition of compatibility

$$\left[\frac{\partial f}{\partial x_j}\right] = \left[\frac{df}{dn}\right] \lambda_j + [f]_{,\alpha} g^{\alpha\beta} x_{j,\beta}, \qquad (A2)$$

where $\delta/\delta t$ is the Thomas δ-derivative, d/dn is the derivative with respect to the normal to the wave surface, G is the normal velocity of the wave surface, λ_j are the components of the unit vector normal to the wave surface, $g_{\alpha,\beta} = x_{i,\alpha} x_{i,\beta}$ are the covariant components of the metric tensor of the wave surface, $x_{i,\alpha} = \partial x_i/\partial u^\alpha$, u^α $\alpha = 1, 2$ are the coordinates on the wave surface, $g^{\alpha\beta}$ are the contravariant components of the metric tensor of the wave surface, in so doing $g^{\alpha\gamma} g_{\beta\gamma} = \delta_\beta^\alpha$, where δ_β^α is the Kroneker's symbol, and $[f]_{,\alpha}$ is the covariant derivative of the discontinuity in the desired function with respect to the surface coordinates u^α.

Formula (A1) is the definition of the Thomas δ-derivative. The validity of (A2) can be shown by sequential multiplication of its right- and left-hand sides by λ_j and $x_{j,\gamma}$ at a time and considering that $\lambda_j x_{j,\gamma} = 0$.

Excluding the value $[df/du]$ from (A1) and (A2) yields

$$\left[\frac{\partial f}{\partial x_j}\right] = -\left[\frac{\partial f}{\partial t}\right] \lambda_j G^{-1} + \frac{\delta[f]}{\delta t} \lambda_j G^{-1} + [f]_{,\alpha} g^{\alpha\beta} x_{j,\beta}. \qquad (A3)$$

Let us chose as the surface coordinates u^1 and u^2, respectively, the straight line coordinate ξ along the generatrices of the wave surface and the arc length s_2 along the directrix line from the wave surface, and consider that $g_{11} = 1$, and $g_{22} \approx 1$ on the whole wave surface ($g_{22} = 1$

only on the line C, but due to the small thickness of this line this equality can be expanded on the whole surface).

Considering the above said, let us rewrite formula (A3) in the form

$$\left[\frac{\partial f}{\partial x_j}\right] = -\left[\frac{\partial f}{\partial t}\right]\lambda_j G^{-1} + \frac{d[f]}{ds_1}\lambda_j + \frac{d[f]}{ds_2}\tau_j + \left[\frac{d(f\xi_j)}{d\xi}\right].$$
$$(A4)$$

During the deduction of (A4) it was also taken into account that

$$\frac{\delta[f]}{\delta t} = \frac{d[f]}{ds_1}\frac{ds_1}{dt} = \frac{d[f]}{ds_1}G,$$

where s_1 is the arc length measured along the ray.

Substituting the function f by $u_{i,(k)} = \partial^k u_i/\partial t^k$ in (A4), we obtain the desired relationship (10).